

11-25-2022

Macro-mesoscopic investigation of cushioning mechanism of recycled concrete aggregate under successive rockfall impacts

Yu-chen SU

College of Mechanics and Materials, Hohai University, Nanjing, Jiangsu 210098, China

Yuan WANG

College of Water Conservancy and Hydropower Engineering, Hohai University, Nanjing, Jiangsu 210098, China

Hui-ming TANG

Faculty of Engineering, China University of Geosciences, Wuhan, Hubei 430074, China

Heng ZHONG

College of Mechanics and Materials, Hohai University, Nanjing, Jiangsu 210098, China

See next page for additional authors

Follow this and additional works at: <https://rocksoilmach.researchcommons.org/journal>



Part of the [Geotechnical Engineering Commons](#)

Custom Citation

SU Yu-chen, WANG Yuan, TANG Hui-ming, ZHONG Heng, LI Xin, LIU Chao-fu, LÜ Ya-ru, . Macro-mesoscopic investigation of cushioning mechanism of recycled concrete aggregate under successive rockfall impacts[J]. Rock and Soil Mechanics, 2022, 43(10): 2698-2706.

This Article is brought to you for free and open access by Rock and Soil Mechanics. It has been accepted for inclusion in Rock and Soil Mechanics by an authorized editor of Rock and Soil Mechanics.

Macro-mesoscopic investigation of cushioning mechanism of recycled concrete aggregate under successive rockfall impacts

Authors

Yu-chen SU, Yuan WANG, Hui-ming TANG, Heng ZHONG, Xin LI, Chao-fu LIU, and Ya-ru L

Macro-mesoscopic investigation of cushioning mechanism of recycled concrete aggregate under successive rockfall impacts

SU Yu-chen¹, WANG Yuan², TANG Hui-ming³, ZHONG Heng¹, LI Xin¹, LIU Chao-fu¹, LÜ Ya-ru¹

1. College of Mechanics and Materials, Hohai University, Nanjing, Jiangsu 210098, China

2. College of Water Conservancy and Hydropower Engineering, Hohai University, Nanjing, Jiangsu 210098, China

3. Faculty of Engineering, China University of Geosciences, Wuhan, Hubei 430074, China

Abstract: Cushion materials can effectively reduce the impact load acting on the rigid protective structures such as shed tunnel and improve the impact resistance of the structures. In order to investigate the variation of cushioning performance of recycled concrete aggregate (RCA) under successive impacts, drop weight impact tests and discrete element simulations are carried out. Test results show that compared with the quartz sand cushion, the transmitted load at the center of concrete shed for RCA under the first impact reduces by 83%, and it is distributed more uniformly. With the increase in the number of impacts, the cushioning performances of both the RCA and quartz sand deteriorate. For the sixth impact, the maximum transmitted loads at the center of concrete shed for RCA and quartz sand are 11.2 times and 1.4 times those of the first impact, respectively. Furthermore, the cushioning performance is strongly influenced by particle shape. The numerical simulation results show that when the proportion of strip particles increases from 0% to 100%, the rotation angle and translation distance of the particles decrease by 40% and 20%, respectively, and the maximum drop weight impact load increases by 37%. The inter-locking effect between particles increases with the irregularity of particle shape, which limits the rotation and translation of the particles, and increases the drop weight impact load and the transmitted load on the concrete slab. The research results may provide theoretical basis and engineering guidance for RCA as a new type of eco-friendly cushion.

Keywords: rockfall; successive impact; cushioning performance; particle shape

1 Introduction

Rockfall disasters occur frequently in mountainous areas of China for a long time and severely threaten socio-economic development and the safety of human life and property^[1]. Cushion materials can effectively reduce the impact load acting on the rigid protective structures such as shed tunnel and improve the impact resistance of the structures^[2–3]. Yuan et al.^[4] carried out the rockfall impact test to investigate the cushioning performance of conventional cushion materials such as gravel, sand and clay. The results showed that clay materials have the best cushioning effect and the greatest reduction in the impact load of rockfalls, followed by sand and gravel. Wang et al.^[5–6] conducted the indoor rockfall impact test to study the influence of compactness on the cushioning performance of sand cushion. The results showed that loose sand cushion has better energy dissipation effect than dense sand cushion. Pei et al.^[7] carried out finite element numerical simulation to study the influence of sand cushion thickness on

cushioning mechanism. The results showed that increasing the thickness of cushion can effectively weaken the influence of rockfall impact on the deformation of shed tunnel roof. The above research showed that granular materials such as sand can effectively absorb the impact energy, reduce the impact load and improve the impact resistance of protective structures.

A large number of studies have shown that particle shape is a key factor affecting the quasi-static mechanical properties of granular materials^[8]. Through the discrete element numerical simulation of large direct shear test, the results show that increasing the irregularity of particles can effectively inhibit the rotation of particles inside the filler, and thus the shear strength of the sample increases as the particle slenderness ratio and angularity index increase^[9–10]. Nie et al.^[11] carried out the discrete element numerical simulation of triaxial shear test, which showed that the smaller the particle sphericity is, the greater the degree of occlusion

Received: 11 October 2021

Revised: 22 June 2022

This work was supported by the Natural Science Foundation of Jiangsu Province (No. BK20200528), the Fundamental Research Funds for the Central Universities (No. B210202103, No. B200202119), the China Postdoctoral Science Foundation (No. 2021M690046) and the National Natural Science Foundation of China (No. 51779264).

First author: SU Yu-chen, male, born in 1991, PhD, Reader, mainly engaged in the research on analysis and control of rockfall hazard. E-mail: wangqs@bjut.edu.cn

Corresponding author: LÜ Ya-ru, female, born in 1987, PhD, Professor, mainly engaged in the research on the rock and soil impact mechanics. E-mail: yaru419828@163.com

between particles is, and the larger the peak friction angle of the sample is. Xu et al.^[12] conducted the research on the irregularity of particle shape and aspect ratio. The results showed that the shear strength of the sample increases with the increases in particle irregularity and aspect ratio. The research results of Wang et al.^[13] also showed that the more irregular the particle shape is, the larger the peak friction angle of the sample is. It can be concluded that the interlocking effect between particles increases with the particle shape irregularity, which significantly changes the quasi-static mechanical properties of the granular cushion materials. However, the effect of particle shape on the dynamic properties of the sample under impact load remains unclear.

To this end, the paper plans to select the cheap and abundant recycled concrete aggregate (RCA) as a new eco-friendly cushion material, and use quartz sand as the comparison material, aiming at investigating the influence of microscopic particle shape on the macroscopic impact resistance performance of cushion. The drop weight impact test is carried out to investigate the variations of cushioning performances of RCA and quartz sand cushions under successive impacts. Discrete element numerical simulation is carried out to understand the influence mechanism of microscopic particle shape on macroscopic impact resistance.

2 Large-scale drop weight impact test

2.1 Test equipment and scheme

The drop weight impact test is conducted at Hohai University to simulate multiple scenarios of successive rockfall impact on shed tunnel roof and cushion. The impact test equipment is composed of steel rail, electric unhooking device, truss structure and drop weight, as shown in Fig. 1. The cushion material is installed in a sand box with dimensions of 1.0 m×1.0 m×0.4 m. The drop weight with a diameter of 0.4 m is made of 304 stainless steel, and it can effectively ensure the consistent test parameters such as impact energy, surface shape and mass of the drop weight under successive impacts. The accelerometer (1B107) is installed on the back of the drop weight with a maximum measuring scale of 200g (g is the gravitational acceleration) and is used to measure the drop weight acceleration during impact. Meanwhile, a concrete slab (1.2 m×1.2 m×0.2 m) is placed at the bottom of the sand box to simulate the shed tunnel roof. Four dynamic stress meters (L1200E) are installed along the vertical central axis, and the

maximum measuring scale is 200 kN. They are used to monitor the distribution of the transmitted load on the concrete slab during the impact process. Before the test, the sample is air-dried and screened, and loaded into a sand box in four layers by vibration compaction, which ensures that the RCA and quartz sand cushions reach the relative compaction of 60% (see Table 1). In addition, in order to improve the efficiency of screening test, three groups of sample particles are randomly selected to carry out screening test to verify the accuracy of grain size distribution curve.

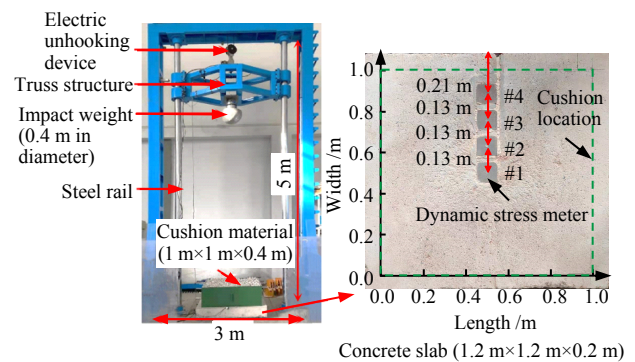


Fig. 1 Front view of drop weight impact test setup

Table 1 Physical properties of RCA and quartz sand

Material	Particle size /mm	Density /($\text{kg} \cdot \text{m}^{-3}$)	d_{50} /mm	C_u	Maximum void ratio	Minimum void ratio	Test void ratio	Relative compaction ratio /%
Quartz sand	0.08–3.7	1 710	1	13.3	0.69	0.36	0.50	60
RCA	20–100	1 340	60	2.4	0.97	0.73	0.83	60

The drop weight impact energy is set as 15 kJ. Before the test, the weight is connected to the electric unhooking device via a truss structure and raised to the designed height. During the test, the unhooking device is activated, and the drop weight falls vertically along the steel frame to impact the center of the cushion. In this study, a high-speed camera (VEO710L) is used to capture the impact process, and 300 frames of images with a resolution of 1 376 pixels × 1 226 pixels can be obtained per second. After the test, the laser range finder is used to measure the surface deformation along the horizontal central axis of the cushion. The measurement interval is 100 mm and the measurement precision is 1.5 mm. After the measurement is completed, lift the weight again to the specified height, repeat the above process, and complete six successive impacts.

2.2 Test results and analysis

2.2.1 Cumulative deformation of cushion

Figure 2 shows the variations of deformation depth

of RCA and quartz sand cushions along the horizontal central axis under successive impacts. The left end of the horizontal central axis of the cushion is located at 0.0 m and the right end is at 1.0 m (see Fig. 1). The initial thickness of RCA cushion is 0.4 m. The maximum deformation depth of the cushion is 0.18 m after the first impact, and the deformation is mainly concentrated between 0.2 m and 0.8 m. Figure 3 shows the distribution of cushion deformation and particle rearrangement under the first impact. One can see that under the first impact, the cushion near the impact point is sunken. Accordingly, the particles are closely arranged and not obviously broken, and the gabion basket is obviously deformed (not broken), which means that the RCA cushion under the first impact mainly dissipates the impact energy through particle rearrangement. For the quartz sand cushion, the maximum deformation depth under the first impact is 0.21 m. It is found that the peak deformation depth of quartz sand cushion is 1.2 times that of RCA cushion, which means that under the same rockfall impact energy, the deformation of quartz sand cushion is much larger than that of RCA cushion. According to the Swiss Highway Committee Specification (ASTRA)^[14], the minimum initial thickness of the cushion is at least twice the maximum deformation depth. As stipulated in the design specification, the minimum thickness of RCA and quartz sand cushions should be 0.36 m and 0.42 m, respectively, which means that the thickness of quartz sand cushion (0.40 m) used in this test is smaller than the designed minimum thickness, thus it tends to cause serious consequences such as failure of protective structure.

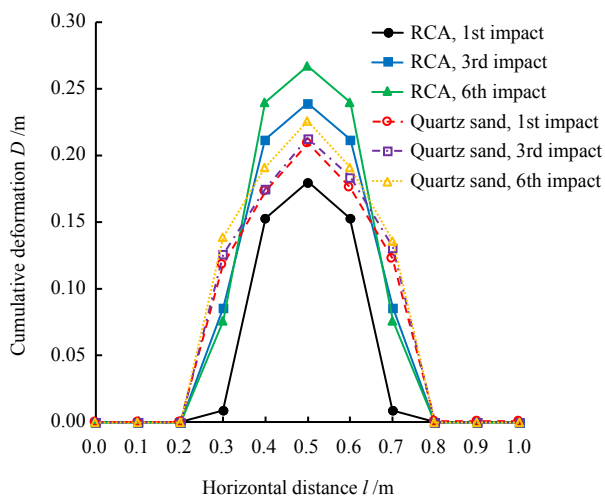


Fig. 2 Variations of cumulative deformation depth of cushion under successive impacts

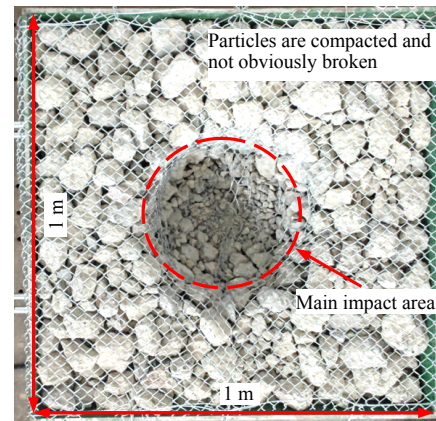


Fig. 3 Top view of deformation of RCA cushion under first impact

After the third and sixth rockfall impacts, the peak deformation depths of RCA cushion reach 0.24 m and 0.27 m, respectively, accounting for 60% and 68% of the initial thickness of the cushion, while the deformation of the cushion is 1.3 times and 1.5 times that after the first impact. The maximum deformation depth of quartz sand cushion under the third and sixth successive impacts is 1.1 times that after the first impact. The increment of deformation depth of quartz sand cushion under successive impacts is less than that of RCA. In engineering practice, when RCA is used as cushion material, it is necessary to consider that the deformation of RCA increases sharply under successive impacts, and the cushioning performance is weakened, resulting in the weakening of the overall impact resistance.

2.2.2 Drop weight impact load

Figure 4 shows the relationships between drop weight impact load and displacement with the number of successive impacts. The impact load is calculated by the product of acceleration and mass (0.6 t), and the displacement is calculated by the quadratic integral of acceleration with respect to time.

Under the first impact, for the RCA cushion, the drop weight impact load versus displacement curve fluctuates obviously. During the impact process, when the impact depth increases to 0.03 m, the drop weight impact load increases rapidly to 31 kN and reaches the first peak and then slightly reduces. With the increase of impact depth, the curve continues to oscillate. When the impact depth increases to 0.19 m, the impact load reaches the peak value of 179 kN and then decays to 0 rapidly. The reason for the fluctuation of the impact load versus displacement curve is that the particle rearrangement occurs in RCA cushion during the impact process, causing the continuous breakage and recombination of the inter-particle force chain.

For the quartz sand cushion, the peak impact load and displacement under the first impact are 86 kN and 0.34 m, respectively. Compared with RCA cushion, the peak impact load of quartz sand cushion reduces by 49% and the peak displacement increases by 17%. This is mainly because the structure of the quartz sand cushion is loose. According to the energy law proposed in the flexible protection system of Bruker company, Switzerland^[16], the larger the deformation during the impact process, the greater the deformation displacement, and the smaller the peak impact load.

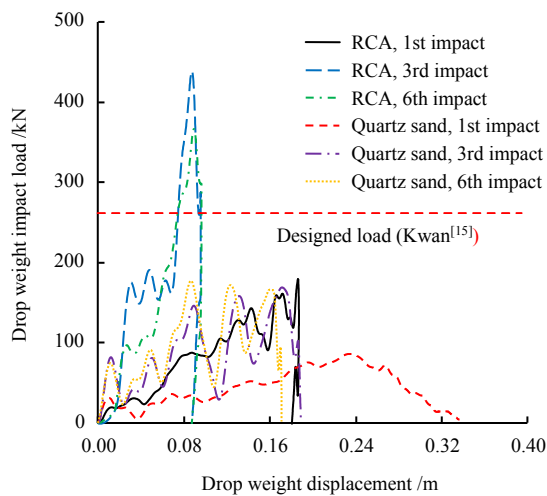


Fig. 4 Variations of cushioning performance under successive impacts

In order to further verify the cushioning performance of RCA cushion material, based on Hertz impact theory^[17] and empirical load reduction factor^[15], the rockfall impact load without cushion protection is calculated by

$$F = 4E / 3R^2 \cdot d^3 \quad (1)$$

where F is the drop weight impact load (kN); E is the effective contact stiffness between cushion material and drop weight; R is the drop weight radius, $R=0.2$ m; and d is the elastic deformation of cushion (m). Through the integration of drop weight impact load by cushion deformation, it is obtained that when the elastic deformation energy is 15 kJ, the corresponding drop weight impact load and elastic deformation are 2 604 kN and 0.014 m, respectively. Using the empirical load reduction factor $K_c=0.1$ proposed by Kwan^[15], the designed load is calculated to be 260.4 kN when the concrete slab is not protected by the cushion. When the RCA and quartz sand are used as cushion materials, the peak value of impact load under the first impact reduces by 32% and 67%, respectively compared with that without cushion protection. This is because a large amount of

plastic deformation occurs in the cushion during the impact process, which prolongs the impact load time history and effectively reduces the peak value of impact load. It also means that using the RCA and quartz sand as cushion materials can effectively improve the impact resistance of shed tunnel structure.

For the RCA cushion, the peak values of the third and sixth impact loads are about 2.5 and 2.0 times that of the first impact, and the initial slope of the impact load versus time history curve increases significantly, and the fluctuation also decreases greatly. Similarly, under the protection of quartz sand cushion, the peak impact loads under the third and sixth impacts are 169 kN and 177 kN, respectively, with increases of 97% and 105% compared to that of the first impact. Meanwhile, the peak displacement of the drop weight reduces by 40% and 48%, respectively. This is because under the action of drop weight impact, the cushion particles are closely arranged due to the rearrangement, the porosity decreases rapidly, the coordination number increases, and the force chain is more stable and not easy to be destroyed. This means that the cushioning mechanism of the cushion particles under the first impact is mainly attributed to rotation and displacement. With the increase of the number of impacts, the remaining thickness of the cushion after the sixth impact reduces to 0.13 m, and the particle rearrangement is greatly reduced by the limitation of remaining pores. There is a great difference in the cushioning mechanism of the cushion material under the first and sixth impacts. It also shows that the cushioning performance of RCA and quartz sand cushions are deteriorated under the successive rockfall impacts.

2.2.3 Distribution of transmitted load on shed tunnel roof

Figure 5 shows the transmitted loads distributed on the retaining wall under the successive drop weight impacts. The abscissa is the ratio of the vertical distance between the dynamic stress gage and the impact center point to the drop weight radius H/R , and the corresponding values of the four stress gages (#1, #2, #3 and #4) on the concrete slab are $H/R=0, 0.65, 1.30$ and 1.95 , respectively (see Fig. 1).

For the RCA cushion under the first impact, the peak transmitted load at the center of shed tunnel roof ($H/R = 0$) is 13.4 kN, and the transmitted load at the edge of the impact area ($H/R = 0.65$) is 12.1 kN. The peak transmitted load at the center is 1.1 times that at the edge, which means that the distribution of the transmitted load within the impact area on the tunnel shed roof (see Fig. 3) is relatively uniform. For the quartz sand cushion, the peak transmitted load under the first impact is 78.9 kN at the center and 5.4 kN at

the edge of the impact area on the tunnel shed roof. The peak value of the transmitted load at the center is 14.6 times that at the edge. Through comparison, it can be found that the peak transmitted load at the center of the RCA cushion is 83% lower than that of the quartz sand cushion, and the good stress diffusion performance makes the impact load more evenly distributed on the tunnel shed roof.

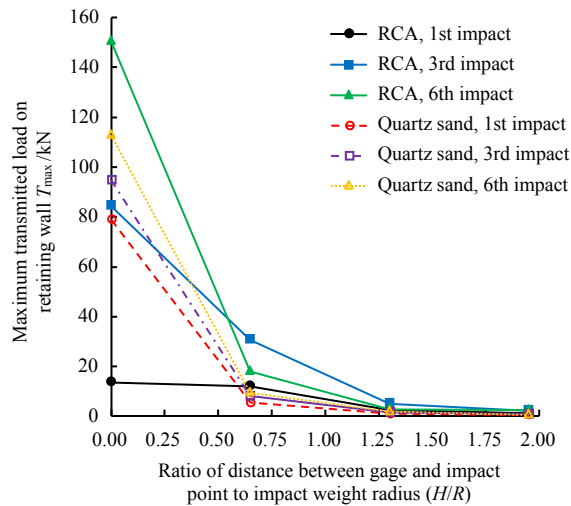


Fig. 5 Distribution of transmitted load on the concrete slab under successive impacts

For the RCA cushion, the peak transmitted load at the center after successive impacts for 3 and 6 times are 84.4 kN and 150.5 kN, respectively, which are 6.3 and 11.2 times that of the first impact. Under the protection of quartz sand cushion, the peak values of transmitted load at the center of shed tunnel roof are 94.8 kN and 112.7 kN, respectively under the third and sixth impacts, which are 1.2 and 1.4 times of the first impact. The cushioning performances of RCA and quartz sand cushions are deteriorated under successive impacts. This is because under successive impacts, the thickness of the remaining cushion is seriously reduced (see Fig. 2), which shortens the distance of the impact load downward transmission. Meanwhile, the cushion particles are closely arranged, the coordination number increases, and the force chain is more stable, resulting in a sharp increase in the transmitted load at the center. In addition, under the sixth impact, the peak transmitted load at the center of the shed tunnel roof protected by the RCA cushion is 8.4 times that of the edge of the impact area. This means that under successive impacts, the thickness of the cushion gradually decreases, the transmitted load on the concrete slab is further concentrated in the central position, and the stress diffusion effect of the cushion is weakened, which increases the risk of rockfall penetrating the shed tunnel structure.

3 Discrete element numerical simulation

3.1 Numerical model and parameters

In order to reveal the influence of cushion particle shape on the cushioning mechanism, a discrete element numerical model is constructed based on PFC3D (particle flow code 3D). In order to reproduce the indoor test as real as possible, we carry out a statistical analysis of the shape of the material used in the test. First, 100 particles are randomly selected from the cushion material, and the particle shape is distinguished by the particle shape parameter, i.e. the flatness ratio $F_1 = d_z/d_y$ and the aspect ratio $E_1 = d_y/d_x$, where d_x , d_y and d_z are the lengths of particle in three mutually perpendicular directions (x , y , z), and d_x and d_z are the longest and shortest edges of particle, respectively.

Figure 6 illustrates the shape classification result of selected particles. It can be found that the aspect ratio and width-to-thickness ratio of the particles are 0.4–1.0. According to the shape classification method proposed by Zingg^[18], the cushion particles are divided into four typical shapes: spheroidal, flat, strip and blade, with the aspect ratio and width-to-thickness ratio of 0.67 as the distinguishing criterion, and the corresponding particle proportions are 43%, 36%, 16% and 5%, respectively. Then, the photographs of the particles are taken from different angles and heights to ensure that the image contains the complete bulge and texture information of the particles. The photographs are imported into the digital image processing software VisualSFM^[19] and MeshLab^[20], and the three-dimensional (3D) point cloud data of the real shape of the particles are generated based on the machine vision technology.

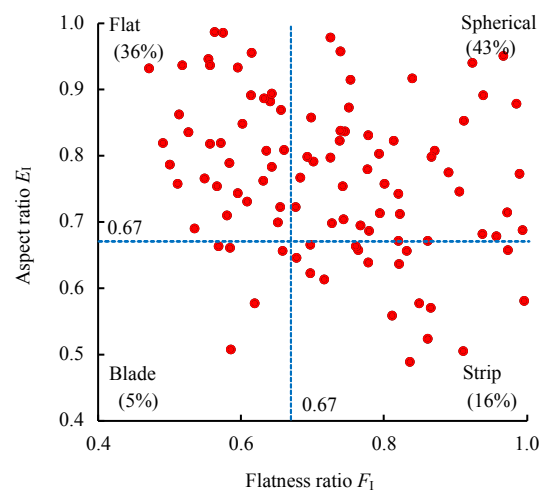



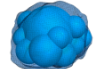

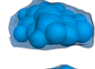

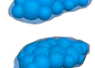


Fig. 6 Particle shape classification

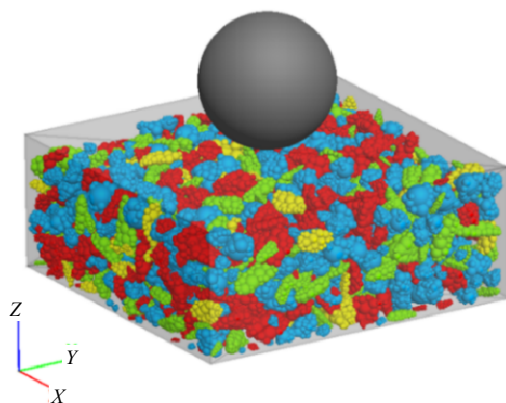
The screening statistics of the cushion particles are conducted before and after the test. Based on the

calculation method of the relative breakage rate B_r proposed by Einav^[21], the limit fractal dimension D is 2.6^[22]. It is found that the relative breakage rate B_r of the RCA cushion particles is only 7.9% after six impacts. This means that the amount of particle breakage during the impact process is small. Therefore, in the discrete element numerical model, the unbreakable particle cluster element (clump) is used to simulate the cushion particle. The microscopic mechanism of impact characteristics of granular material is revealed from the aspects of contact force between particles, particle rotation and particle translation.

In the numerical model, based on the 3D point cloud data of particle shape, the bubblepack^[23] algorithm is used to fill the 3D geometric boundary and reconstruct the clump-based 3D model. The specific shape parameters are listed in Table 2. Using the pluviation method, samples are generated according to the particle size distribution and the initial relative density of the drop weight test (see Fig. 7).

Table 2 Summary of clumps adopted in discrete element model

Particle shape	Real particle	Clump model	Aspect ratio E_1	Flatness ratio F_1	Proportion /%
Spheroidal			0.99	0.79	43
Flat			0.71	0.50	36
Strip			0.41	0.75	16
Blade			0.57	0.43	5



Note: Red indicates spheroidal particle, green indicates strip particle, blue indicates flat particle, and yellow indicates blade particle.

Fig. 7 3D discrete element model of drop weight impact test

The Hertz contact model is used for the contact analysis between particles^[23], and the microscopic parameters in the discrete element model are calibrated by the trial-and-error method. The calibrated microscopic

mechanical parameters are shown in Table 3. In order to improve the efficiency of discrete element numerical calculation, the alternative method mentioned by Bourrier et al.^[24] and Su et al.^[25] is employed, i.e. the wall element is used to simulate the gabion net in the drop weight impact test. One side of the wall in contact with the particles is set as the active surface, and the other side is set as the inactive surface, which can ensure that there is no contact between the wall and the drop weight during the impact process. The role of the wall is to limit the upward movement of particles, and the diffusion effect of the gabion net on the impact load of rockfall is ignored. After the cushion sample is established according to 1:1 indoor drop weight test, the initial drop weight speed (7.1 m/s) is set, and the cushion material is impacted with 15 kJ energy to numerically simulate the drop weight impact test. In order to better reveal the influence of particle shape on the microscopic mechanism of cushion, five groups of discrete element numerical simulations are carried out (see Table 4). By changing the proportion of spheroidal and strip particles, the influence of particle shape on the cushioning mechanism is revealed. These tests are labeled B100E0, B75E25, B50E50, B25E75 and B0E100, and the corresponding proportions of spheroidal particles are 100%, 75%, 50%, 25% and 0%, and the proportions of strip particles are 0%, 25%, 50%, 75% and 100%.

Table 3 Microscopic mechanical parameters used in discrete element model

Density /($\text{kg} \cdot \text{m}^{-3}$)	Cushion void ratio	Shear modulus between contacted particles /MPa	Poisson's ratio between contacted particles	Friction coefficient between contacted particles	Damping coefficient
2350	0.45	80	0.25	0.5	0.01

Table 4 Summary of numerical simulation cases

Test No.	Proportion of particles with different shapes /%			
	Spheroidal	Strip	Flat	Blade
B100E0	100	0	0	0
B75E25	75	25	0	0
B50E50	50	50	0	0
B25E75	25	75	0	0
B0E100	0	100	0	0

3.2 Numerical validation

The discrete element numerical simulation of drop weight impact test is carried out, and the experimental results of impact load and center transmitted load of concrete slab are compared with the simulation results (see Fig. 8). It can be found that the peak values of drop weight impact load obtained from the experiment

and numerical simulation are 179 kN and 156 kN, respectively. The difference between the experimental and numerical results is less than 15%. Therefore, it is considered that the numerical model can accurately simulate the drop weight impact test. Meanwhile, the transmitted load at the center of the concrete slab is compared between the experimental and numerical results, and the numerical result is 19% larger than the experimental result. In addition, the fluctuation of the time-history curves of the drop weight impact load and the retaining wall transmitted load is greater than that of the numerical result. This may be because the clump used in the numerical model does not consider the particle breakage during the impact process, which makes the force chain formed between the particles in the numerical simulation more stable, resulting in a larger impact load transmitted to the concrete slab. Figure 9 shows the time-history curves of average rotation angle and translation distance of spheroidal and strip particles during the impact process. One can see that the change trend of strip and spheroidal particles is consistent, both reaching the peak value at 0.02 s, and the peak rotation angle of strip particles is 1.3 times that of spheroidal particles. This is because the more irregular the particle shape is, the greater the degree of occlusion between particles is, which limits the rotation angle of particles during impact. However, the difference of translation distance between strip and spheroidal particles is only 5%, which indicates that the influence of particle shape change on particle rotation angle is more significant than that of translation distance. In order to further quantitatively reveal the effect of particle shape on the rearrangement mechanism, a detailed quantitative study on the proportion of particles with different shapes is conducted below.

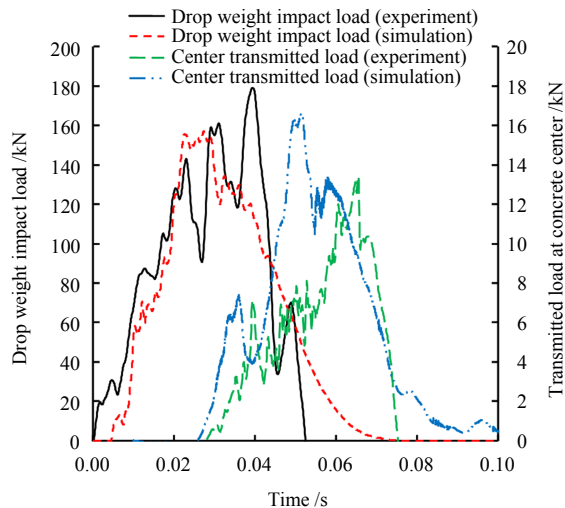


Fig. 8 Comparisons between experimental and numerical results

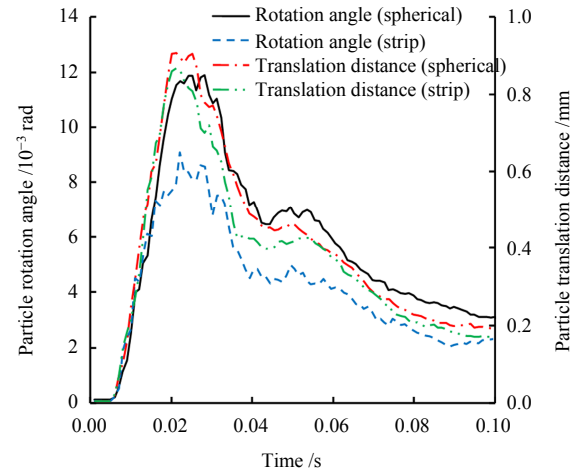


Fig. 9 Time-history curves of rotation angle and translation distance of spheroidal and strip particles

3.3 Influence mechanism of particle shape on cushioning performance

Figure 10 shows the influence of proportion of the strip particle on the particle rotation angle and translation distance. The peak value of average rotation angle of particles decreases by 16%, 28%, 36% and 39%, respectively, as the proportion of strip particles increases by 25% (see Fig. 10(a)). The peak value of average translation distance of particles decreases by 14%, 12%, 13% and 21%, respectively, as the proportion of strip particles increases by 25% (see Fig. 10(b)). This means that the particle rotation angle and translation distance decrease with the increase of particle shape irregularity during the impact process. It is further verified that the more irregular the particle shape, the greater the degree of occlusion between particles, which limits the rearrangement of particles and reduces the cushioning performance of the cushion material.

The influence of the overall irregularity on the cushioning performance is studied by increasing the proportion of strip particles in the cushion (0%, 25%, 50%, 75% and 100%), as shown in Fig. 11. It can be found that as the proportion of strip particles increases, the peak value of drop weight impact load increases significantly. When the proportion of strip particles increases from 0% to 100%, the peak impact load increases by 37% accordingly. It is also found that the rotation angle and translation distance of the particles reduce by 40% and 20%, respectively. It shows that the increase of particle irregularity limits the rearrangement of particles during impact, thus reducing the cushioning performance of cushion material. Therefore, in practical engineering, particles with regular shape can further reduce the impact load of rockfall and improve the overall impact resistance of protection engineering.

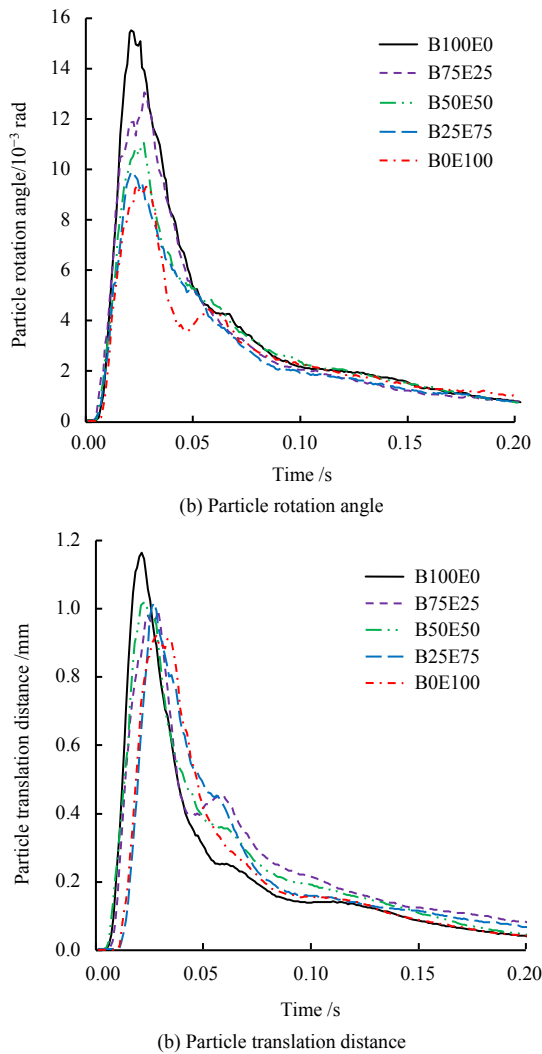


Fig. 10 Influence of strip particle proportion on particle rearrangement

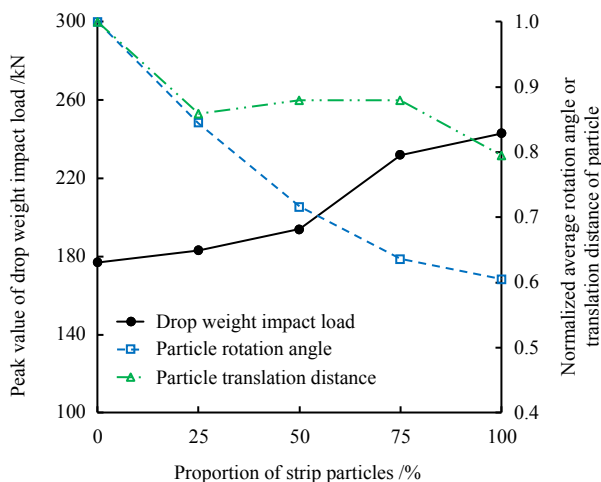


Fig. 11 Influence of particle shape on cushioning performance and particle rearrangement

4 Conclusions

Through drop weight impact test and discrete element numerical simulation, the cushioning performance and particle rearrangement mechanism of RCA and quartz

sand cushions under successive impacts are studied. The main conclusions are drawn as follows:

(1) Compared with the quartz sand cushion, the RCA cushion under the first impact can better reduce the transmitted load acting on the shed tunnel roof, and the load distribution is more uniform. After using the RCA cushion, the peak value of transmitted load at the center of shed tunnel roof reduces by 83% compared with the quartz sand cushion. Meanwhile, the peak value of the transmitted load at the center under the protection of the quartz sand cushion is 14.6 times that at the edge, while the peak value of the transmitted load at the center under the RCA cushion is only 1.1 times that at the edge.

(2) Under successive impacts, the cushioning performance and stress diffusion performance of the RCA and quartz sand cushions are deteriorated. For the RCA, the peak values of the transmitted load at the center of the shed tunnel roof under the third and sixth impacts are 6.3 and 11.2 times that of the first impact, respectively. For the quartz sand cushion, they are 1.2 and 1.4 times that of the first impact, respectively. This means that under successive impacts, the thickness of the cushion gradually decreases, the transmitted load on the concrete slab is further concentrated in the central position, and the stress diffusion effect of the cushion is weakened.

(3) The more irregular the shape of cushion particles, the greater the degree of occlusion between particles during impact, which significantly limits the particle rearrangement and reduces the cushioning performance of cushion material. When the proportion of strip particles increases from 0% to 100%, the peak values of particle rotation angle and translation distance decrease by 40% and 20%, respectively, and the peak value of drop weight impact load increases by 37%.

References

- [1] HE Si-ming, WU Yong, LI Xin-po. Research on restitution coefficient of rock fall[J]. *Rock and Soil Mechanics*, 2009, 30(3): 623–627.
- [2] WANG Dong-po, HE Si-ming, OUYANG Chao-jun, et al. Study of dynamic response of shed reinforced concrete slab to impact load of rock-fall[J]. *Rock and Soil Mechanics*, 2013, 34(3): 881–886.
- [3] WU Yong, HE Si-ming, LI Xin-po, et al. Study on elliptic anti rock-fall impact structure with double energy dissipation layers wrapping up pier eccentrically in mountains[J]. *Engineering Mechanics*, 2017, 34(10): 158–167.
- [4] YUAN Jin-ke, HUANG Run-qiu, PEI Xiang-jun. Test

- research on rock-fall impact force[J]. *Rock and Soil Mechanics*, 2014, 35(1): 48–54.
- [5] WANG Dong-po, HE Si-ming, GE Sheng-jin, et al. Mountain hazards induced by the earthquake of Sep. 07, 2012 in Yiliang and the suggestions of disaster reduction[J]. *Journal of Mountain Science*, 2013, 31(1): 101–107.
- [6] WANG Dong-po, ZHOU Liang-kun, PEI Xiang-jun, et al. Experimental and numerical study on rockfall impacts on sand-soil cushions[J]. *Journal of Vibration and Shock*, 2020, 39(18): 195–202.
- [7] PEI Xiang-jun, LIU Yang, WANG Dong-po. Study on the energy dissipation of sandy soil cushions on the rock-shed under rockfall impact load[J]. *Journal of Sichuan University*, 2016, 48(1): 15–22.
- [8] BIAN Xue-cheng, LI Wei, LI Gong-yu, et al. Three-dimensional discrete element analysis of railway ballast's shear process based on particles' real geometry[J]. *Engineering Mechanics*, 2015, 32(5): 64–75.
- [9] HUA Wen-jun, XIAO Yuan-jie, WANG Meng, et al. Discrete element modeling (DEM) study on effect of gradation and morphology on shear strength behavior of rock debris as embankment fill materials[J]. *Journal of Central South University (Science and Technology)*, 2021, 52(7): 2332–2348.
- [10] WU Jian-qi, LI Lei, WANG Jun. Dynamic shear characteristics of interface between different geosynthetics and recycled concrete aggregate[J]. *Journal of Vibration and Shock*, 2022, 41(1): 279–287.
- [11] NIE Z, FANG C, GONG J, et al. Exploring the effect of particle shape caused by erosion on the shear behaviour of granular materials via the DEM[J]. *International Journal of Solids and Structures*, 2020, 202: 1–11.
- [12] XU M Q, GUO N, YANG Z. Particle shape effects on the shear behaviors of granular assemblies: irregularity and elongation[J]. *Granular Matter*, 2021, 23(2): 1–15.
- [13] WANG Yun-jia, SONG Er-xiang, ZHANG Qian-li. DEM analysis of the aggregate shape effect on mechanical properties of rockfill[J]. *Engineering Mechanics*, 2022, 39(3): 137–146.
- [14] ASTRA. Effects of rockfall on protection galleries[S]. Berne, Switzerland: Federal Roads Office, 2008.
- [15] KWAN J S H. Supplementary technical guidance on design of rigid debris-resisting barriers (GEO Rep. No. 270)[R]. Hong Kong: Geotechnical Engineering Office, 2012.
- [16] LABIOUSE V. Experimental study of rock sheds impacted by rock blocks[J]. *Structural Engineering International Journal*, 1996, 3(1): 171–175.
- [17] SU Y, CHOI C E. Effects of particle shape on the cushioning mechanics of rock-filled gabions[J]. *Acta Geotechnica*, 2020, 275: 105724.
- [18] ZINGG T. Beitrage zur schootteranalyse[J]. *Schweizerische Mineralogische und Petrographische Mitteilungen*, 1935, 15: 39–140.
- [19] STALMACH O, SAPIETOVA A, DEKYS V, et al. Conversion of data from the laser scanner to the ANSYS Workbench[J]. *MATEC Web of Conferences*, 2019, 254: 02003.
- [20] SCHOLLEMAN F, PEREIRA C B, ROSENHAIN S, et al. An anatomical thermal 3D model in preclinical research: combining CT and thermal images[J]. *Sensors*, 2021, 21(4): 1200.
- [21] EINAV I. Breakage mechanics—part I: theory[J]. *Journal of the Mechanics and Physics of Solids*, 2007, 55(6): 1274–1297.
- [22] ZHU Sheng, DENG Shi-de, NING Zhi-yuan, et al. Gradation design method for rockfill materials based on fractal theory[J]. *Chinese Journal of Geotechnical Engineering*, 2017, 39(6): 1151–1155.
- [23] Itasca. Particle flow code in three dimensions[M]. Minneapolis, Minnesota: Itasca Consulting Group, Inc., 1999.
- [24] BOURRIER F, LAMBERT S, HEYMANN A, et al. How multi-scale approaches can benefit the design of cellular rockfall protection structures[J]. *Canadian Geotechnical Journal*, 2011, 48(12): 1803–1816.
- [25] SU Y, CHOI C E, LV Y R, et al. Towards realistic simulations of the impact dynamics of boulders on rock-filled gabion: combined effects of natural rock shapes and crushing[J]. *Engineering Geology*, 2021, 283: 106026.